

AD-A099 034

MASSACHUSETTS INST OF TECH LEXINGTON LINCOLN LAB  
LINEAR FILTERING MODELS FOR TERRAIN IMAGE SEGMENTATION. (U)  
FEB 81 C W THERRIEN

F/G 14/5

F19628-80-C-0002

UNCLASSIFIED

TR-552

ESD-TR-80-245

NL

1 OF 1  
AD A  
098034



**LEVEL**

13

AD A099034

**Technical Report**

**552**

**C.W. Therrien**

**Linear Filtering Models for Terrain  
Image Segmentation**

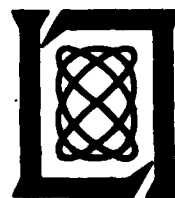
**4 February 1981**

Prepared for the Department of the Air Force  
under Electronic Systems Division Contract F19628-80-C-0002 by

**Lincoln Laboratory**

**MASSACHUSETTS INSTITUTE OF TECHNOLOGY**

**LEXINGTON, MASSACHUSETTS**



Approved for public release; distribution unlimited.

**DTIC**

**MAY 18 1981**

81 5 18<sup>A</sup> 085

DTIC FILE COPY

The work reported in this document was performed at Lincoln Laboratory, a center for research operated by Massachusetts Institute of Technology, with the support of the Department of the Air Force under Contract F19628-80-C-0002.

This report may be reproduced to satisfy needs of U.S. Government agencies.

The views and conclusions contained in this document are those of the contractor and should not be interpreted as necessarily representing the official policies, either expressed or implied, of the United States Government.

This technical report has been reviewed and is approved for publication.

FOR THE COMMANDER

*Raymond L. Loiselle*

Raymond L. Loiselle, Lt. Col., USAF  
Chief, ESD Lincoln Laboratory Project Office

Non-Lincoln Recipients

**PLEASE DO NOT RETURN**

Permission is given to destroy this document  
when it is no longer needed.

MASSACHUSETTS INSTITUTE OF TECHNOLOGY  
LINCOLN LABORATORY

6 LINEAR FILTERING MODELS FOR TERRAIN IMAGE SEGMENTATION

(12) Chao, W. / THERRIEN  
Group 27

14  
17-0000

(11) TECHNICAL REPORT 552

(11) 4 FEB 1981

(12) 27

13, F17668-02 1-10-81

Approved for public release; distribution unlimited.

(18) 1-10-81 17-0000

LEXINGTON

MASSACHUSETTS

2076

### Abstract

A method for modeling images of natural terrain is developed and applied to the segmentation of aerial photographic data. An underlying stochastic structure based on linear filtering concepts provides a means of modeling the terrain in local areas of the image. Superimposed on this is a Markov random field that describes transitions from regions of one terrain type to another. Maximum likelihood and maximum a posteriori estimation is applied to estimate regions of similar terrain. Results of application to digitized aerial photographs of a rural area are presented and discussed.

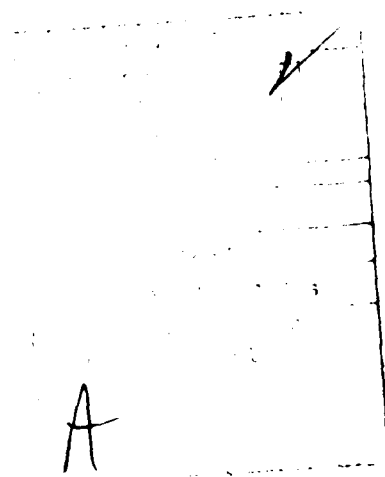


## Table of Contents

	<u>Page</u>
Abstract	iii
I. Introduction	1
II. Linear Filtering Models for Images	3
III. Segmentation as a Region Estimation Problem	9
IV. Results of Segmentation	13
V. Conclusions	21
References	22

## I. INTRODUCTION

The segmentation of images is a vital part of image analysis for a host of applications. Where specific models for images are lacking, one is forced to base the analysis on heuristic arguments and heuristically motivated features and performance can be evaluated only on an empirical basis. Much of the work in image analysis has fallen into this category. When one is able to restrict the class of images so that specific models can be developed, the resulting analysis algorithms are placed on a much firmer foundation and their performance can be evaluated from both analytical and empirical considerations. We have taken the latter approach in this report.

Many images of natural terrain can be effectively characterized as two-dimensional (2-D) random processes. The segmentation of these images into areas of known types is important for a variety of applications including military surveillance and reconnaissance, crop and land use data collection, and cartography. In addition, many images other than those of terrain contain areas of texture that can be well modeled by random processes. This report describes a model for images based on stochastic linear filtering concepts. Using this model, one can develop the probability density functions for the image data. Segmentation of the image is then treated as an estimation problem and the resulting algorithms have a clear intuitive interpretation.

Earlier results of this research as applied to texture data were reported in Reference 1. This report extends those results and demonstrates their application to terrain image data. While no claim of universality is made, the algorithms have been effective in segmenting aerial photographs of rural terrain and provide encouragement for continued research along these lines.

In the following section, we postulate a general class of linear filtering models and then specialize the results somewhat for the work covered in this report. Next, we consider segmentation as a region estimation problem and

develop maximum likelihood (ML) and maximum a posteriori (MAP) estimates for the regions (segments). Finally, we present some results of application of the ML and MAP algorithms to aerial photographic data and discuss and compare the two approaches.



## II. LINEAR FILTERING MODELS FOR IMAGES

A. In this section, we consider models for an image of the form

$$F'(n,m) = \sum_{\alpha} a_{ij} F'(n-i, m-j) + \sum_{\beta} b_{ij} W(n-i, m-j) \quad (1a)$$

$(i,j) \neq (0,0)$

$$F(n,m) = F'(n,m) + G \quad (1b)$$

$$n \in [0, N-1]$$

$$m \in [0, M-1]$$

where  $\alpha$  and  $\beta$  are finite-extent masks covering the filtered points,  $W(n,m)$  are a set of independent identically distributed zero mean random variables, and  $G$  is a constant representing the mean value of the image. In general,  $G$  could be made a function of the image coordinates  $(n,m)$  but this implies a form of non-stationarity and an associated registration problem. Since the images to be dealt with are (at least locally) stationary, we shall not make that generalization.

In the following, it will be assumed that  $\alpha$  and  $\beta$  are chosen so that  $F'$  is recursively computable [2,3] given  $W$  and vice versa. This will lead to simplifications in the analysis to follow.

If the vectors  $\underline{f}$ ,  $\underline{w}$ , and  $\underline{g}$  represent an ordered set of the corresponding array points (derived for example by scanning rows of the image), then Eq. (1) can be written in a matrix formulation as

$$A(\underline{f}-\underline{g}) = B \underline{w} + \underline{\gamma} \quad (2)$$

where  $A$  and  $B$  are matrices whose non-zero elements are derived from the terms  $a_{ij}$  and  $b_{ij}$  in Eq. (1) and  $\underline{\gamma}$  represents a set of boundary conditions imposed by the finite extent of the image. In general, these boundary conditions should be modelled as random variables or the parameters of the model should

be made space-varying over the region where the spatial masks  $\alpha$  and  $\beta$  are not fully contained within the boundaries of the image (see Ref. 4 for a discussion of this problem with respect to 1-D signals). The inclusion of these effects, however, is of little significance in most problems of practical interest and merely serves to complicate the analysis. Thus, it is convenient to set the boundary conditions  $\underline{y}$  to  $\underline{0}$  and accept the approximation that results. Since the terms  $W(n,m)$  are independent, one can solve Eq. (2) for  $\underline{w}$  and express the multivariate probability density function for the image as

$$p_{\underline{f}}(\underline{f}) = \frac{1}{|A^{-1}B|} p_{\underline{w}}(B^{-1}A(\underline{f}-\underline{g}))$$

$$= \prod_{\substack{(N-1, M-1) \\ (n,m)=(0,0)}} p_w(E(n,m)) \quad (3)$$

where the notation  $E(n,m)$  is used to represent the ordered components of the vector  $B^{-1}A(\underline{f}-\underline{g})$  and where we have used the fact that since both  $A$  and  $B$  correspond to recursively computable masks, their determinants are equal to one. Further, since mask  $\beta$  has a recursive form,  $E(n,m)$  can be computed from

$$E(n,m) = -\sum_{\substack{\beta \\ (i,j) \neq (0,0)}} b_{ij} E(n-i, m-j) - \sum_{\alpha} a_{ij} F'(n-i, m-j) \quad (4)$$

Equation (3) provides a formula for the probability density function of image  $F$  in terms of the probability density function for the driving variables  $W(n,m)$  and is key to the estimation theoretic approaches that are taken in this report. Later, explicit forms for the filter and the density  $p_w$  will be assumed and more specific results based on these forms will be derived. However, the methods just discussed are capable of representing only images with homogeneous properties such as an image of a single type of terrain\*. The images to be considered for segmentation contain a number of different homogeneous regions. Thus, it is necessary to add another level of structure to the model to represent these more typical images. This topic will be discussed next.

B. Consider an image such as that depicted in Figure 1 consisting of regions  $R_1, R_2, \dots, R_p$ . It will be assumed that within each region, the image can be represented by a model of the type discussed in Part A. Denote the probability density function for the driving terms in a region  $R_i$  of type  $k_i$  by  $p_{k_i}(\cdot)$ . Note that there may be more than one region of a given type. Then, ignoring boundary effects, we can express the probability density for the image, given the regions  $R_1, \dots, R_p$  as

$$p(F|R_1, \dots, R_p) = \left( \prod_{(n,m) \in R_1} p_{k_1}(E_{k_1}(n,m)) \right) \cdot \left( \prod_{(n,m) \in R_2} p_{k_2}(E_{k_2}(n,m)) \right) \cdot \dots \cdot \left( \prod_{(n,m) \in R_p} p_{k_p}(E_{k_p}(n,m)) \right) \quad (5)$$

---

\* In this report, we shall refer to images whose statistical characteristics are spatially invariant as "stationary" and use the term "homogeneous" only in a loose intuitive sense. Thus, the word homogeneous should not be confused with the mathematical property used in the literature on random fields.

106512-N

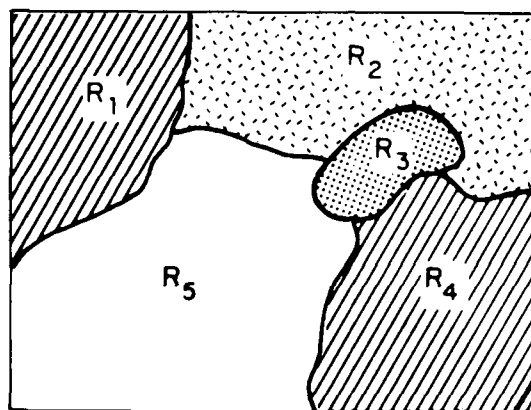


Fig. 1. Image consisting of homogeneous regions.

106513-N

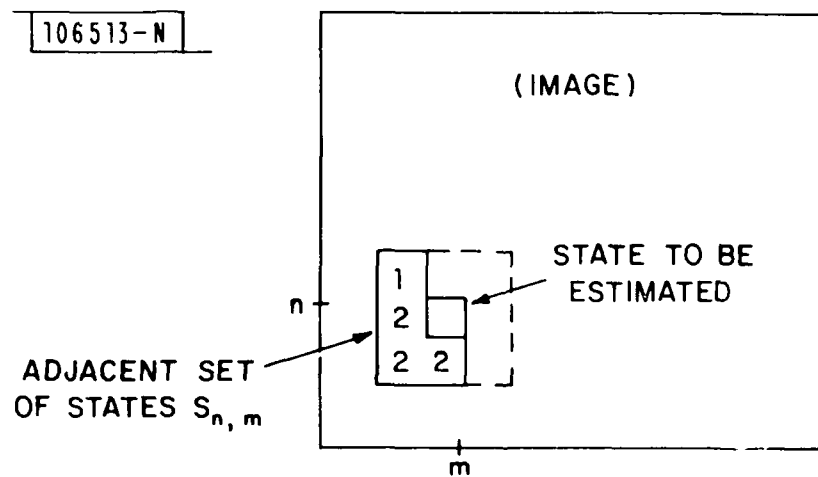


Fig. 2. Illustration of state dependencies for Markov chain.

where the subscript  $k_i$  on the residual terms  $E(n,m)$  indicates that these terms were computed using the filter of type  $k_i$ . Equation (5) or its logarithm can be used as a likelihood function to generate maximum likelihood estimates for the regions. This procedure will be detailed in section III. However, maximum likelihood estimation implicitly assumes that all region configurations are equally likely and this is seldom the case for most images. In reality, regions for a given class of images may be more likely to be of some approximate size and density and it is not unusual to have some rough prior information about the occurrence of regions within the image. When such prior information is available, a better procedure is to use some form of Bayes estimation. This can be approached as follows.

Let the occurrence of regions within an image be modeled through region transition statistics. In particular, define the "state"  $s(n,m)$  of a point  $(n,m)$  as the region type to which that point has been assigned. Thus, if there are  $K$  region types, the state may take on values in the set of integers  $\{1,2,\dots,K\}$ . Next, assume that the state of a point is stochastically dependent on some adjacent set of states in a support region  $S_{n,m}$  (see Fig. 2). In particular, following Kaufman *et al.* [5], we shall assume for the moment that the states form a Markov chain specified by transition probabilities  $\Pr[s(n,m)|S_{n,m}]^*$ . The Markov chain imposes constraints on the shape of the state support region. For example, the symmetric region indicated by the dashed lines in Figure 2 is not allowed. We shall relax the constraint on  $S_{n,m}$  later by allowing the probabilistic structure of the states to have other Markov dependencies. However, the Markov chain assumption will permit development of the estimation equations for the state assignments in a straightforward manner. Since the set of all possible state assignments is one to one with the set of all possible divisions of the image into regions, we shall have reached our objective.

---

\* Our notation is convenient but may be somewhat confusing. A proper (but more cumbersome) notation would be  $\Pr[s(n,m)=s_0|S_{n,m}=S_0]$  where  $s_0$  is an integer in the set  $\{1,2,\dots,K\}$  and  $S_0$  is composed of integers in the same set. Thus, when we write  $\Pr[1|S_{n,m}]$  as in Eq. (14), the reader should interpret this as  $\Pr[s(n,m)=1|S_{n,m}=S_0]$ .

Let  $S$  represent a particular set of state assignments for all points in an image. Our goal is to evaluate  $\Pr[S]$ . If the image is  $N$  by  $N$  pixels in size, then let the pixels be numbered from 1 to  $N^2$  according to the ordering imposed by the Markov chain. Then we can write

$$\begin{aligned}\Pr[S] &= \Pr[s_{N^2}, s_{N^2-1}, \dots, s_1] \\ &= \Pr[s_{N^2} | s_{N^2-1}, \dots, s_1] \cdot \Pr[s_{N^2-1} | s_{N^2-2}, \dots, s_1] \cdots \Pr[s_2 | s_1] \cdot \Pr[s_1]\end{aligned}\tag{6}$$

Let  $S_k$  be the support region for  $s_k$ . Then when  $S_k$  is completely within the boundary of the image, we have  $\Pr[s_k | s_{k-1}, \dots, s_1] = \Pr[s_k | S_k]$ . When  $S_k$  is not completely within the image boundary, i.e., when  $s_k$  does not have full support, we shall approximate  $\Pr[s_k | s_{k-1}, \dots, s_1]$  by a term of the same form where zeros are inserted for the states not present. Thus, Eq. (6) can be expressed as

$$\Pr[S] = \prod_{k=1}^{N^2} \Pr[s_k | S_k] = \prod_{\substack{(n,m) \\ \text{in image}}} \Pr[s(n,m) | S_{n,m}]\tag{7}$$

Equations (5) and (7) can be combined to develop conditions for the maximum a posteriori estimates of the state assignments which define the regions. This is discussed in the next section.

### III. SEGMENTATION AS A REGION ESTIMATION PROBLEM

The basic concepts for approaching segmentation as a region estimation problem were developed in the previous section. In this section, we will restrict attention to a particular class of linear filtering models and develop some more specific results.

The assumptions that are made in the following are that the model of Eq. (1) is purely autoregressive so that  $b_{ij} = \delta_{ij}$  (the Kronecker delta), that the mask  $\alpha$  has a quarter plane causal form, i.e.,  $a_{ij}$  is non-zero only for  $i \in [0, I]$  and  $j \in [0, J]$  and that the  $W(n, m)$  are Gaussian with density function

$$p(w) = \frac{1}{\sqrt{2\pi}\sigma} \exp\left(-\frac{w^2}{2\sigma^2}\right) \quad (8)$$

For the causal autoregressive model, the filter coefficients can be efficiently computed using the algorithm described in Reference 6.

Taking minus twice the log of Eq. (5) and applying Eq. (8) we obtain

$$\begin{aligned} -2 \ln p(F|R_1, R_2, \dots, R_P) &= \sum_{R_1} \left[ \frac{E_{k_1}^2(n, m)}{\sigma_{k_1}^2} + \ln \sigma_{k_1}^2 \right] + \dots \\ &+ \sum_{R_P} \left[ \frac{E_{k_P}^2(n, m)}{\sigma_{k_P}^2} + \ln \sigma_{k_P}^2 \right] - N^2 \ln 2\pi \\ &= \sum_{i=1}^P \sum_{(n, m) \in R_i} \left[ \frac{E_{k_i}^2(n, m)}{\sigma_{k_i}^2} + \ln \sigma_{k_i}^2 \right] - N^2 \ln 2\pi \quad (9) \end{aligned}$$

For the maximum likelihood procedure, the number of regions  $P$  and the regions themselves are assumed to be deterministic parameters of the density function. An ML estimate for these parameters is obtained by choosing values that maximize Eq. (5) or, equivalently, minimize Eq. (9). A moment's reflection indicates that Eq. (9) is minimized if every point  $(n,m)$  in the image is assigned to a region  $R_i$  or type  $k_i$  such that the term in brackets is minimum. For the case of two region types (but possibly multiple regions), we are led to a segmentation rule of the form

$$\frac{E_1^2(n,m)}{\sigma_1^2} + \ln \sigma_1^2 \stackrel{\textcircled{1}}{<} \frac{E_2^2(n,m)}{\sigma_2^2} + \ln \sigma_2^2 \quad (10)$$

where the number above or below the inequality indicates the region type to which the point  $(n,m)$  will be assigned if the inequality holds.

Since the ML method leads to a decision rule that assigns points to region types without regard to the assignment of adjacent points, one might expect this segmentation rule to produce a number of false assignments leading to a somewhat "spotty" result. The examples in the next section show that this is in fact the case. The main advantage of the ML method is that it is quick and easy to apply. The spottiness of the result can sometimes be removed by lowpass filtering.

An improved form of region estimation is Bayes estimation where the regions are treated not as unknown parameters, but as random quantities whose statistical properties are described by the Markov transition model developed in the previous section. In particular, we will consider maximum a posteriori (MAP) estimation where we maximize the probability of a given set of regions conditioned on our observation of the image. From Bayes rule, the a posteriori probability can be written as

$$\Pr[R_1, R_2, \dots, R_P | F] = \frac{p(F | R_1, R_2, \dots, R_P) \Pr[R_1, R_2, \dots, R_P]}{p(F)} \quad (11)$$



Since the denominator is not a function of the regions, it is only necessary to be concerned with the terms in the numerator. Observe, first, that since the set of all possible region assignments for an image is one-to-one with the set of all possible state assignments for the pixels, the second term in the numerator of Eq. (11) is given by Eq. (7). Next, observe that the double summation in Eq. (9) can be written as

$$\sum_{i=1}^P \sum_{(n,m) \in R_i} \left[ \frac{E_{k_i}^2(n,m)}{\sigma_{k_i}^2} + \ln \sigma_{k_i}^2 \right] = \sum_{\text{all } (n,m)} \frac{E_{s(n,m)}^2(n,m)}{\sigma_{s(n,m)}^2} + \ln \sigma_{s(n,m)}^2 \quad (12)$$

Now, taking minus twice the log of Eq. (11), using Eqs. (7), (9) and (12), and eliminating the constant terms, we find the MAP estimate requires that the pixel states be chosen to minimize

$$\sum_{\text{all } (n,m)} \left[ \frac{E_{s(n,m)}^2(n,m)}{\sigma_{s(n,m)}^2} + \ln \sigma_{s(n,m)}^2 - 2 \ln \Pr[s(n,m) | S_{n,m}] \right] \quad (13)$$

This requires that each term in the sum be separately minimized. In the case of two region types, this reduces to the conditions

$$\frac{E_1^2(n,m)}{\sigma_1^2} + \ln \sigma_1^2 - 2 \ln \Pr[1 | S_{n,m}] \stackrel{\textcircled{1}}{<} \frac{E_2^2(n,m)}{\sigma_2^2} + \ln \sigma_2^2 - 2 \ln \Pr[2 | S_{n,m}] \quad (14)$$

Since the states are assumed to form a Markov chain, Eqs. (13) or (14) can be solved for the states recursively according to the ordering of the chain.

The segmentation algorithms as thus far developed have the characteristic that all of the processing of the image to effect the segmentation is directional. Since many terrain images have no preferred direction, it is desirable to perform operations on the image which are omni-directional. Unfortunately, 2-D filters whose outputs are recursively computable do not allow for this symmetry. However, under certain conditions, it is possible to allow the Markov transition probabilities to be defined for a symmetric state support region. Such models have been studied in the context of Markov Random Fields [7-9].

In the case of a symmetric state support region, Eqs. (13) or (14) can no longer be solved recursively. Solution by direct methods for any reasonably sized images appears to be hopeless since all of the  $N^2$  states are coupled through nonlinear equations. However, the equations can be solved by iteration as follows. An initial set of states, usually the maximum likelihood states, are assigned to the image points. The Markov transition probabilities in Eqs. (13) or (14) are then based on these state assignments and held fixed while the equations are evaluated to determine a new set of states. These new state estimates are now inserted into the equations and the procedure is repeated in an iterative manner. If a stage of iteration is reached where the state assignments no longer change, then the MAP estimate has been found. If such a stage is not reached, this may be an indication that the transition probabilities are inconsistent and should be redefined. This solution procedure bears some resemblance to relaxation labeling techniques [10,11] in that the state assignments are iteratively updated by considering the state assignments of neighboring pixels. In practice, the procedure has been found to converge typically after 10 to 20 iterations.

#### IV. RESULTS OF SEGMENTATION

Figure 3(a) shows a digitized aerial photograph of a rural area containing some trees and fields. The digitized image is 128 by 128 pixels in size with gray levels represented on a scale of 0 to 255 (8 bits). It was desired to segment the image into two regions corresponding to the trees and fields without further distinguishing between different types of trees or fields. The data used to design the 4 by 4 pixel whitening filters for each image class are shown in the white boxes. The resulting filters were then applied to the entire image to perform the segmentation.

The result of ML segmentation is shown in Figure 3(b) where points in the image that were assigned to tree regions are coded as black and points assigned to field regions are coded as white. Although the true tree and field regions are perceptually discernible, the result is very "spotty". In fact, the ML estimate consists of not two but a multiplicity of smaller regions. This result is not surprising based on our earlier observations about the ML estimate.

Figure 3(c) shows the MAP segmentation of the same scene. For this and the remaining examples, the transition probabilities were taken to be proportional to the number of black or white pixel assignments in a square region surrounding the given pixel. In this case, the state support region was taken to be 9 by 9 pixels and the number of iterations used was 16. The MAP result clearly shows the effect of the transition probabilities in providing connectivity in the region estimates. There are only a relatively small number of isolated misclassified points. For practical purposes, these points can be eliminated and the area near the boundary can be made smooth by post filtering. This will be illustrated in a later example.

Figure 4(a) shows another image consisting of regions of fields and trees. Figure 4(b) shows the MAP segmentation of this image using the filters designed for the scene of Figure 3(a). It is not surprising that the result is not perfect because there are some significant differences in the gray tones

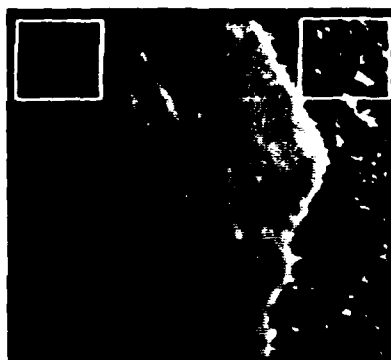


Fig. 3. Segmentation of an image into regions of trees and fields:  
 (a) Digitized aerial photograph (128 by 128 pixels) showing training data (b) ML segmentation (c) MAP segmentation.



(a)



(b)

Fig. 4. Segmentation of another tree and field image using filters designed on data Fig. 3(a): (a) Digitized photograph (128 by 128 pixels) (b) MAP segmentation.

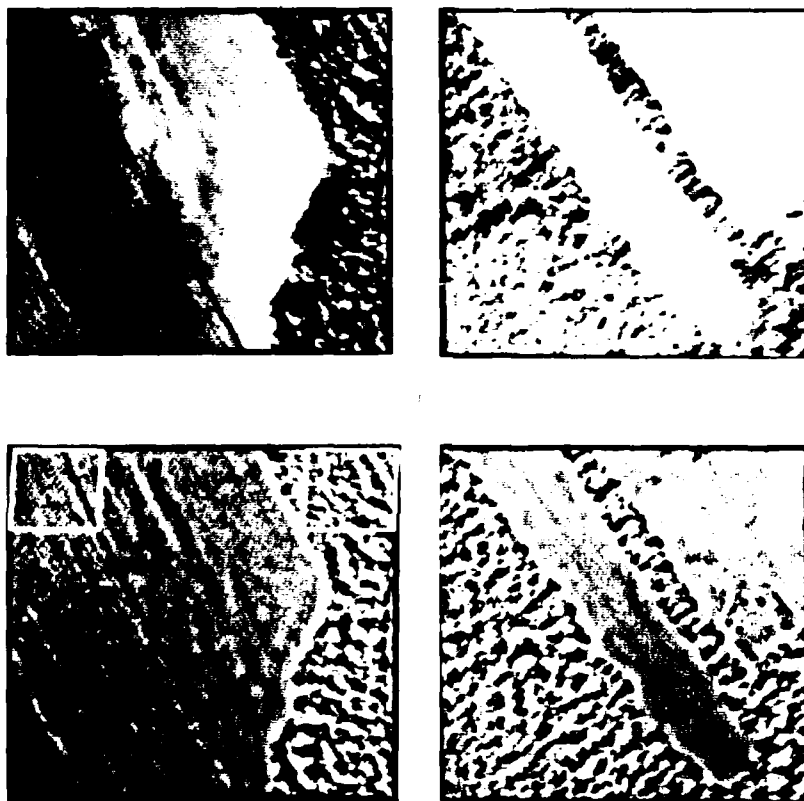
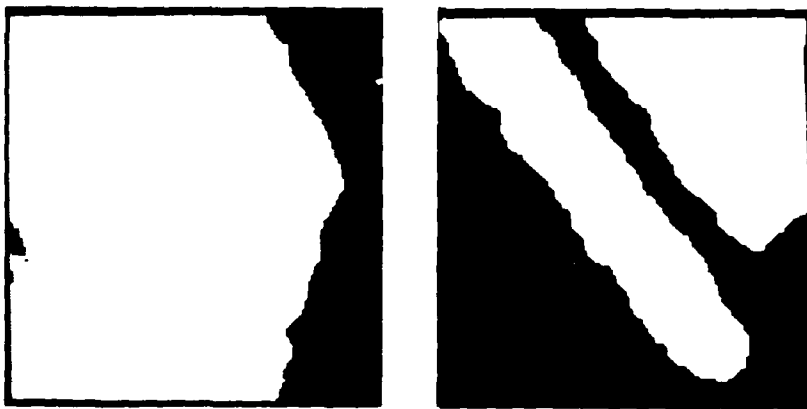


Fig. 5. Steps in segmentation of two images of trees and fields:  
(a) Original digitized images (b) Preprocessed images show training data for MAP segmentation.



(c)



(d)

Fig. 5. Steps in segmentation of two images of trees and fields:  
 (c) MAP segmentation of preprocessed images (d) MAP segmentation  
 after post median filtering.

of each class between the two original images. The problem can be alleviated by preprocessing both images prior to segmentation to render the average tonal value in local regions a middle gray. The preprocessing involves median filtering to minimize artifacts in the boundary regions between terrain segments followed by mean filtering to insure that the result will be close to a middle gray. In particular, the preprocessed image  $H$  is defined by the equations

$$H'(n,m) = F(n,m) - \underset{\mathcal{R}}{\text{Median}}\{F(n,m)\}$$

$$\Delta(n,m) = \frac{1}{M} \sum_{\mathcal{R}} H'(n,m)$$

$$H(n,m) = H'(n,m) - \Delta(n,m) + \frac{T_{\max} + 1}{2}$$

where  $\mathcal{R}$  is a small region surrounding the point  $(n,m)$ ,  $M$  is the number of points in  $\mathcal{R}$  and  $T_{\max}$  is the largest tonal value in the image representation, i.e., that corresponding to pure white. For these experiments,  $\mathcal{R}$  was taken to be a square region 11 by 11 pixels in size and  $T_{\max}$  was equal to 255. This preprocessing is a modified version of a more general procedure that can be used in various applications to locally expand or compress image contrast [12].

Figure 5 shows the steps involved in segmentation of the two images. Figure 5(a) shows the two original images. Figure 5(b) shows the preprocessed images with the data used for filter design shown in the white boxes. Figure 5(c) shows the MAP segmentation results and Figure 5(d) shows the final segmentation results after post median filtering. Except for a small area on the left border of the left hand image (probably due to some local image abnormality not compensated for by the preprocessing) the final results show a clean and accurate segmentation of the images.



Another experiment involved further segmentation within one of the segments determined in the previous experiments. The area of consideration is shown in the white box in Figure 6(a) and enlarged in Figure 6(b). Within the tree region, two types of textures can be discerned which correspond to small and large trees. Figure 7(a) shows the MAP segmentation of the tree area where the large trees are coded in black and the remainder of the image is coded in white. The boundary is outlined in gray and superimposed in white on the original image in Figure 7(b). The result was found to be very accurate when compared to human perception of the tree boundary on the original photographic data.

At the time of this report, experiments involving more than two classes of terrain have not been performed. However, the two-class experiments described suggest that segmentation might well be carried out in a hierarchical layered form where an initial segmentation into gross categories is first performed and then additional segmentation is performed within the segments as necessary. Further experiments will have to be conducted to determine the trade-offs between such a layered approach and the direct segmentation into a number of classes in a single step.

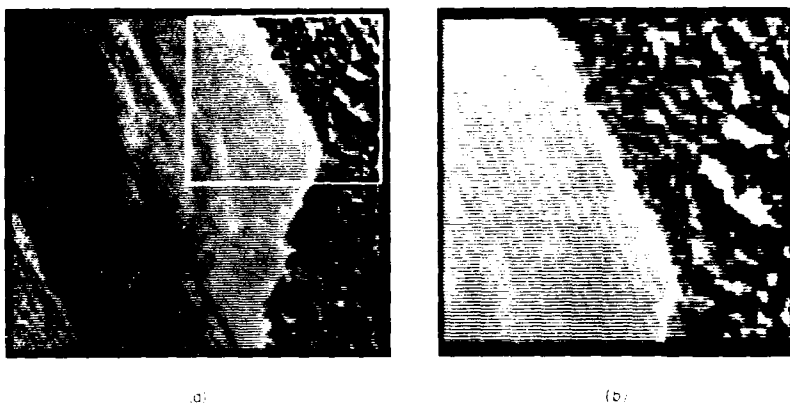


Fig. 6. Photograph used for tree segmentation experiment:  
 (a) Original digitized image (b) Enlarged section of image  
 used for experiment.

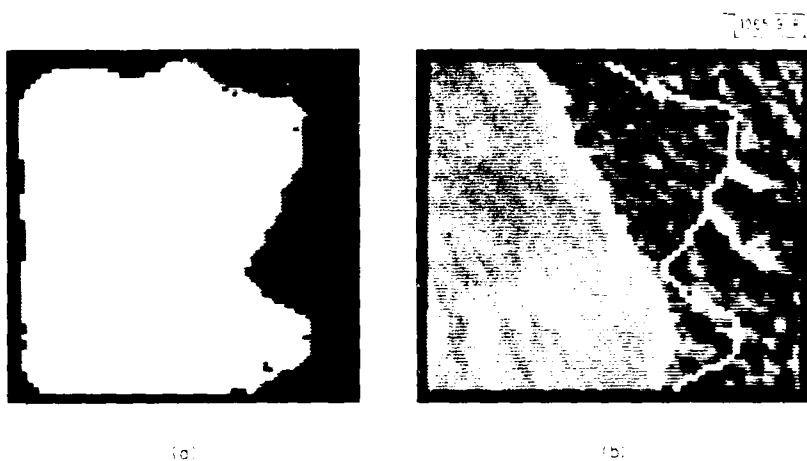


Fig. 7. MAP segmentation for tree region of Fig. 6(b):  
 (a) MAP segmentation (b) Image with superimposed tree  
 boundary.

## V. CONCLUSIONS

The segmentation of arbitrary images is a difficult problem because of the wide diversity of image data and the corresponding difficulty to establish models of sufficient generality. When the class of images can be restricted, model development is more feasible and segmentation algorithms can be designed that have a firm theoretical foundation. Images of natural terrain form such a class and their segmentation is an important aspect of automated image analysis for reconnaissance and surveillance, cartography and other similar applications.

This report described a class of models for terrain images with two levels of structure. The underlying structure is based on stochastic filtering concepts and provides a means of representing the texture-like quality in local regions of terrain. Superimposed on this structure is a Markov random field that describes transitions from one region type to another.

Using the models developed here, we considered segmentation as a region estimation problem and explored maximum likelihood and maximum a posteriori estimation procedures. The ML approach ignores the Markov structure that describes the occurrence of regions and yields an algorithm which is simple to apply but produces "spotty" results. The MAP approach leads to a set of conditions that must be solved by iteration but produces a more connected and generally more desirable result. Examples of both procedures were given on aerial photographic data of natural terrain. The examples suggested that segmentation could be effectively carried out with a layered strategy beginning with a gross segmentation of the image and proceeding to more detailed levels of segmentation within the original segments. Further research would be necessary to study the trade-offs involved in this approach versus an approach that segments the image into many different categories in a single step.

#### REFERENCES

- [1] C.W. Therrien, "Linear Filtering Models for Texture Classification and Segmentation," Proc. 5th Intl. Conf. on Pattern Recognition, Miami, FL 1-4 December 1980.
- [2] R.M. Mersereau and D.E. Dudgeon, "Two-Dimensional Digital Filtering," Proc. IEEE, 64 (1975).
- [3] D.E. Dudgeon, "Pecursibility of Two-Dimensional Difference Equations," Quarterly Progress Report 113, Research Laboratory of Electronics, M.I.T., Cambridge.
- [4] C.W. Therrien, "A Sequential Approach to Target Discrimination," IEEE Trans. Aerospace Electron. Systems AES-14, 433 (1978).
- [5] H. Kaufman, J.W. Woods, V.K. Ingle, R. Mediavilla and A. Radpour, "Recursive Image Estimation: A Multiple Model Approach," Proc. 18th Conf. on Decision and Control, Fort Lauderdale, FL 12-14 December 1979.
- [6] C.W. Therrien, "Relations Between 2-D and Multichannel Linear Prediction," IEEE Trans. Acoust., Speech, and Signal Processing (to be published).
- [7] M. Hassner and J. Sklansky, "The Use of Markov Random Fields as Models of Texture," Computer Graphics and Image Processing, 12, 357 (1980).
- [8] L.N. Kanal, "Markov Mesh Models," Computer Graphics and Image Processing, 12, 371 (1980).
- [9] J. Besag, "Spatial Interaction and the Statistical Analysis of Lattice Systems," J. Royal Statistical Society 36, 192.
- [10] A. Rosenfeld, R.A. Hummel, and S.W. Zucker, "Scene Labeling by Relaxation Operations," IEEE Trans. Syst., Man., Cybern., SMC-6, 420 (1976).
- [11] R.A. Hummel and S.W. Zucker, "On the Foundations of Relaxation Labeling Processes," Proc. 5th Intl. Conf. on Pattern Recognition, pp. 50-63, Miami, FL 1-4 December 1980.
- [12] T. Peli and J.S. Lim, "Adaptive Filtering for Image Enhancement," Proc. 1981 Intl. Conf. on Acoustics, Speech, and Signal Processing, Atlanta March 30-April 1, 1981.

UNCLASSIFIED

SECURITY CLASSIFICATION OF THIS PAGE (When Data Entered)

REPORT DOCUMENTATION PAGE		READ INSTRUCTIONS BEFORE COMPLETING FORM
1. REPORT NUMBER ESD-TR-80-245	2. GOVT ACCESSION NO. AD A099034	3. RECIPIENT'S CATALOG NUMBER
4. TITLE (and Subtitle)  Linear Filtering Models for Terrain Image Segmentation		5. TYPE OF REPORT & PERIOD COVERED  Technical Report
7. AUTHOR(s)  Charles W. Therrien		6. PERFORMING ORG. REPORT NUMBER Technical Report 552
9. PERFORMING ORGANIZATION NAME AND ADDRESS Lincoln Laboratory, M.I.T. P.O. Box 73 Lexington, MA 02173		8. CONTRACT OR GRANT NUMBER(s)  F19628-80-C-0002
11. CONTROLLING OFFICE NAME AND ADDRESS Air Force Systems Command, USAF Andrews AFB Washington, DC 20331		10. PROGRAM ELEMENT, PROJECT, TASK AREA & WORK UNIT NUMBERS  Program Element No. 627021 Project No. 4594
14. MONITORING AGENCY NAME & ADDRESS (if different from Controlling Office)  Electronic Systems Division Hanscom AFB Bedford, MA 01731		12. REPORT DATE 4 February 1981
		13. NUMBER OF PAGES 30
		15. SECURITY CLASS. (of this report)  Unclassified
		15a. DECLASSIFICATION DOWNGRADING SCHEDULE
16. DISTRIBUTION STATEMENT (of this Report)  Approved for public release; distribution unlimited.		
17. DISTRIBUTION STATEMENT (of the abstract entered in Block 20, if different from Report)		
18. SUPPLEMENTARY NOTES  None		
19. KEY WORDS (Continue on reverse side if necessary and identify by block number)  segmentation                      terrain image analysis 2-D filtering                      2-D autoregressive models Markov random fields		
20. ABSTRACT (Continue on reverse side if necessary and identify by block number)  A method for modeling images of natural terrain is developed and applied to the segmentation of aerial photographic data. An underlying stochastic structure based on linear filtering concepts provides a means of modeling the terrain in local areas of the image. Superimposed on this is a Markov random field that describes transitions from regions of one terrain type to another. Maximum likelihood and maximum a posteriori estimation is applied to estimate regions of similar terrain. Results of application to digitized aerial photographs of a rural area are presented and discussed.		

UNCLASSIFIED

SECURITY CLASSIFICATION OF THIS PAGE (When Data Entered)

DATE  
FILMED  
-8